https://doi.org/10.56295/1ACEG09

APPLICATION OF A COPULA APPROACH TO QUANTIFY RAINFALL-INDUCED ROCKFALL

Farshad Bahootoroody[1], Davide Ettore Guccione[1], Klaus Thoeni[1], Anna Giacomini[1]
[1]*Centre for Geotechnical Science and Engineering, The University of Newcastle, Callaghan, NSW 2308, Australia.*

ABSTRACT

Rockfall hazards threaten coastal infrastructure, particularly under high rainfall conditions that accelerate slope degradation. This paper presents a copula-based statistical analysis of the relationship between rainfall and rockfall volume at Susan Gilmore Beach, Newcastle, NSW, Australia. Over a two-year monitoring period, drone-based photogrammetry surveys captured volumetric changes across 28 time intervals. To emphasise larger, more hazardous events, the 75th percentile of daily rainfall was paired with the 75th percentile of observed rockfall volumes. Correlation measures (Pearson's r and Kendall's τ) indicated moderate to strong dependencies, prompting assessment of three Archimedean copulas (Gumbel, Clayton, and Frank). Goodness-of-fit tests identified the Gumbel copula as the best model for capturing upper-tail dependence, linking high rainfall to substantial rockfall volumes. Joint and conditional probabilities derived from the copula framework revealed that extreme precipitation markedly elevates the likelihood of significant rockfalls, surpassing insights from conventional linear correlation. The findings underscore the value of nonlinear, tail-focused statistical approaches in hazard characterisation. The conditional probability provides explicit likelihoods of specific rockfall volumes for given rainfall amounts, offering the potential to define risk thresholds and inform targeted mitigation strategies. By integrating high-resolution 3D monitoring with an advanced copula-based model, this study provides a robust methodological template for analysing rainfall-triggered instability in coastal cliff environments.

Keywords: rockfall hazard assessment, probabilistic analysis, copula modelling, conditional probability

1 INTRODUCTION

Rockfall hazards pose risks to infrastructure and public safety, as sudden collapses can endanger lives and disrupt transport corridors and facilities. This risk is particularly relevant in Australia, where extensive coastal cliffs vary in lithology and height. Intense rainfall is a well-established trigger for rockfalls (Delonca et al., 2014). Climate change exacerbates the urgency of this issue, as extreme rainfall events are projected to increase in frequency and intensity, potentially amplifying cliff retreat and instability (Contino et al., 2017; Ansari et al., 2015; Melillo et al., 2020; Vessia et al., 2020). Therefore, precisely understanding the rainfall–rockfall relationship is crucial for hazard mitigation planning and climate resilience in these vulnerable coastal zones.

Recent studies have increasingly focused on enhancing rockfall prediction models and climate impact assessments (Matsuoka, 2019; Nissen et al., 2021; Leyva et al., 2022; Birien and Gauthier, 2023; Malsam and Walton, 2024; Mirhadi and Macciotta, 2023). The lack of comprehensive and high-resolution historical rockfall datasets and insufficient records of weather conditions at the time of failure have made it difficult to establish clear relationships between weathering processes and rockfall occurrence. This challenge is further compounded by the inaccessibility of hazardous slopes, inconsistencies in monitoring techniques, geological variability, and limitations in data precision and temporal coverage. These constraints are particularly problematic for short-term analyses that require detailed, high-frequency observations.

Despite advances in remote sensing and monitoring techniques, establishing robust correlations between rainfall and rockfall occurrence remains challenging. Studies relied primarily on cross-correlation or simple linear models (Delonca et al., 2014; Leyva et al., 2022; Bajni et al., 2021), often with limited temporal resolution and qualitative volume estimates. More recent investigations (Birien and Gauthier, 2023; Malsam and Walton, 2024) have employed high-resolution, lidar-derived data and terrestrial laser scanning (TLS) to track thousands of discrete rockfall events over shorter intervals. Although these efforts have shed light on the role of rainfall, temperature, and weathering, the underlying relationships can exhibit strong nonlinearity and tail-dependent behaviour that conventional correlation measures (e.g., Pearson's coefficient) fail to capture. In most studies, correlation analyses, often using the Pearson correlation coefficient, assess linear relationships between normally distributed variables (Schober et al., 2018; Hazra and Gogtay, 2016). However, this method fails to capture nonlinear dependencies, common in climatology, where data distributions are skewed (Schoelzel and Friederichs, 2008). Schirmacher and Schirmacher (2008) and Hashemi et al. (2015) highlighted its limitations, showing that different dependence structures can yield identical coefficients, leading to misleading conclusions.

To address these limitations, copula-based modelling offers a flexible framework for describing complex, nonlinear dependence structures in geotechnical data (Nelsen, 2007; Ningrum et al., 2017). Unlike linear correlation, copulas provide a means of isolating and quantifying how extreme rainfall events coincide with large-volume rockfalls—a phenomenon referred to as "tail dependence." This approach has found success in various risk assessment contexts, including landslide hazard evaluation (Motamedi and Liang, 2014; Li et al., 2018) and slope stability analyses (Wu, 2015; Wang and Li, 2018). Nonetheless, applications of copula theory to short-term, high-resolution rockfall datasets remain relatively scarce, underscoring the need for further exploration.

Against this backdrop, the current study aims to quantify the rainfall–rockfall volume relationship at Susan Gilmore Beach (SGB) in Newcastle, NSW, Australia, using a copula-based statistical approach recently proposed by the authors (Bahootoroody et al., 2025). Rainfall, among other factors such as freeze–thaw cycles, thermal fluctuations, wave action resulting in undercutting, root jacking from vegetation growth and geological conditions, has been identified as one potential rockfall trigger. In the current study, rainfall has been chosen as the primary trigger to illustrate the application of copula theory. While the proposed approach can accommodate the inclusion of other triggers in future research, it currently serves as a foundational step. This initial focus allows for a thorough evaluation of the method's applicability and effectiveness before expanding its scope to include additional triggers. Over a two-year period (2022–2024), high-resolution drone photogrammetry surveys were performed to capture volumetric changes resulting from rockfalls across 28 time intervals. The research objectives are threefold: (1) to characterise the magnitude and frequency of rockfalls using refined 3D data acquisition; (2) to assess the suitability of various copula families (Gumbel, Clayton, and Frank) in modelling rainfall-driven rockfall dependence; and (3) to leverage joint and conditional probabilities to improve hazard assessment. By integrating advanced geospatial monitoring with rigorous statistical modelling, this study demonstrates how nonlinear dependence insights can inform more targeted and effective risk management strategies for coastal cliff instability.

2 METHODOLOGY

This study employs a novel copula-based approach to model the dependency between rockfall volume and rainfall (Bahootoroody et al., 2025). The methodology of the copula-based approach is briefly reported here. Full details of each step can be found in Bahootoroody et al. (2025). Copula modelling is a powerful statistical approach for capturing dependencies between variables by constructing joint distributions from their marginal distributions. Unlike traditional multivariate models, copulas provide flexibility in defining dependence structures (Genest and Favre, 2007).

According to Sklar's theorem (1959), for any two random variables, U and V, with a joint cumulative distribution function (CDF) denoted as $H(u, v)$, there exists a copula function C that links their marginal distributions:

$$H(u,v) = C(F_U(u), F_V(v)) \quad (1)$$

where F_U and F_V represent the marginal CDFs of U and V, respectively. This relationship generalises to higher dimensions, allowing the construction of a multivariate dependence structure while preserving the individual behaviour of each variable (Embrechts et al., 2001). Figure 1 illustrates the structured methodology used to estimate the conditional probability of rockfall volume based on rainfall, employing a copula-based approach. The process is divided into two main stages: Data Processing and copula Fitting.

The first stage begins with data collection (Step 1), where rainfall and rockfall volume datasets are gathered. Next, the dataset is split into training and validation subsets (Step 2) to ensure a robust model evaluation. Subsequently, an Empirical Cumulative Distribution Function (ECDF) is constructed (Step 3) to analyse the distribution characteristics of the variables. These distributions are then transformed into a standard uniform distribution (Step 4), enabling compatibility with copula modelling. Finally, correlation measures such as Pearson's correlation and Kendall's tau are computed (Step 5) to quantify the relationship between the variables.

The second stage, copula Fitting, starts with selecting the most suitable copula function (Step 6) to model the variables' dependence structure. The goodness-of-fit of the chosen copula is assessed (Step 7) to ensure an appropriate model fit. Once validated, the copula joint probability distribution is constructed (Step 8), allowing for a comprehensive probabilistic representation of the relationship between rainfall and rockfall volume. In the final step, the conditional probability of rockfall volume given rainfall is estimated (Step 9), providing critical insights into hazard assessment. The entire process is implemented through a Python script explicitly developed for this research, ensuring computational efficiency and reproducibility.

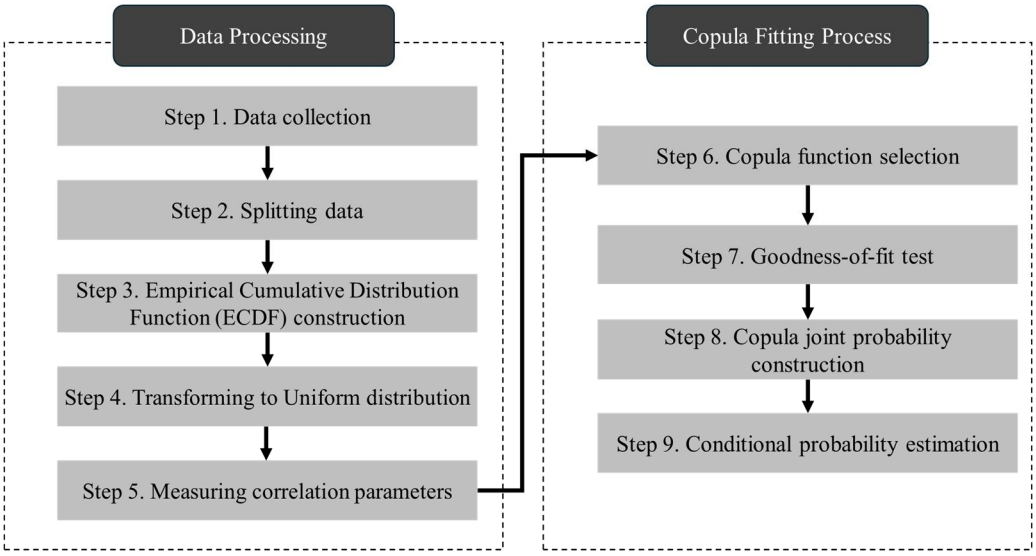

Figure 1. The schematic overview of the copula-based framework details data processing and copula fitting for conditional probability estimation.

2.1 DATA PROCESSING

The data processing stage prepares the dataset for copula modelling by transforming raw data into a format suitable for dependency analysis. This involves data collection, dataset splitting, distribution transformation, and correlation assessment.

The process begins with data collection (Step 1), where the variables of interest are obtained. Further details on data sources and characteristics are provided in Section 4.1. After collection, the dataset is split into training and testing subsets (Step 2) using an 80:20 ratio, where 80% of the data is used for copula modelling, while the remaining 20% is allocated for estimating conditional probability. A stratified random sampling approach is applied to ensure that both subsets maintain representative characteristics (Tippett, 1931).

To facilitate copula-based dependency modelling, the Empirical Cumulative Distribution Function (ECDF) is constructed (Step 3) for each variable. The ECDF is a non-parametric method that estimates the cumulative probability distribution based on observed data (Bernards et al., 2020; Parzen, 1962). Since copula modelling requires uniform marginals, the empirical cumulative distribution function (ECDF) is applied to transform the raw data variables into a uniform distribution:

$$\hat{F}_{(u)} = \frac{1}{n}\sum_{i=1}^{n} I(U_i \leq u) \tag{2}$$

where I is an indicator function that equals 1 if $U_i \leq u$ and 0 otherwise. The transformation is applied to obtain uniform variables u and v in the unit interval [0,1] (Step 4), which is essential for copula modelling, as it allows dependency structures to be analysed independently of their marginal distributions (Papaefthymiou and Kurowicka, 2009; Bedford and Cooke, 2001).

Following this, correlation parameters are computed (Step 5) to quantify the relationship between variables. Pearson's correlation coefficient is employed to measure linear dependence (Embrechts et al., 2001), while Kendall's tau (Kendall, 1938) is used to assess monotonic associations, offering a nonparametric alternative suitable for capturing nonlinear dependencies (Nelsen, 2007).

This stage establishes a structured foundation for copula fitting and conditional probability estimation by transforming the dataset into a uniform scale and quantifying dependencies.

2.2 COPULA FITTING PROCESS

The copula fitting stage establishes the dependency between variables by selecting an appropriate copula function, validating its effectiveness, constructing the joint probability distribution, and deriving conditional probabilities. The process begins with choosing a copula function (Step 6), which defines how the relationship between the variables is modelled. Copulas are classified into different families, with two primary categories commonly used in statistical modelling: elliptic and Archimedean copulas. Archimedean copulas were selected for this study due to their established application in modelling rainfall patterns (Wang et al., 2017; Ma et al., 2013; Zhang and Singh, 2019; Villarini et al., 2008). This family includes the Clayton, Frank, and Gumbel, which provide different ways to capture dependency patterns, including strong lower or upper tail dependencies. The dependence copula parameter θ is estimated based on

Kendall's tau (τ). Table 1 summarises the mathematical relationship between θ and τ in three Archimedean copulas (Sepúlveda-García and Alvarez, 2022).

Table 1. Copula density function c in a bivariate case, for some popular Archimedean copulas used in geotechnics, and simplified relationships between Kendall's tau (τ) and the copula parameter (θ) (modified after Sepúlveda-García and Alvarez (2022).

Copula	$C(u, v; \theta)$	Relationship $\tau - \theta$
Frank	$-\frac{1}{\theta}\ln\left[1+\frac{\left(e^{-u\theta}-1\right)\left(\mathrm{e}^{-v\theta}-1\right)}{\mathrm{e}^{-\theta}-1}\right]$	$\tau = 1-\frac{4}{\theta}+4\frac{D_1(\theta)}{\theta}$
Gumbel	$\exp\left[-\left((-\ln u)^{\theta}+(-\ln v)^{\theta}\right)^{1/\theta}\right]$	$\tau = 1-\frac{1}{\theta}$
Clayton	$\left[u^{-\theta}+v^{-\theta}-1\right]^{-\frac{1}{\theta}}$	$\tau = \frac{\theta}{2+\theta}$

The selection of an appropriate copula is based on the characteristics of the dataset and the type of relationship observed. Following the selection, a goodness-of-fit evaluation (Step 7) determines how well the chosen copula represents the data. This is achieved using the Akaike Information Criterion (AIC) (Akaike, 1974) and Bayesian Information Criterion (BIC)(Schwarz, 1978), which assesses the trade-off between model complexity and fit quality. These metrics are defined as follows:

$$AIC = 2k - 2l \tag{3}$$

$$BIC = k\ln N - 2\ln l \tag{4}$$

where l is the likelihood function, k is the number of model parameters, and N is the sample size. The copula function yielding the lowest AIC and BIC values is considered the best fit for the dataset. Once the copula function is validated, the joint probability distribution is formulated (Step 8). This step constructs both the copula probability density function (PDF) and the cumulative distribution function (CDF), which collectively define the dependence between variables. These distributions offer insight into the probability of joint occurrences, revealing key patterns such as clustering and tail dependencies. To enhance interpretability, graphical representations such as contour plots and 3D surface plots can be generated to visualise how probability distributions change across different values of the variables.

Finally, the conditional probability of one variable given another is estimated (Step 9). This probability quantifies the likelihood of rockfall occurring for a given level of rainfall and is derived using the copula model. Mathematically, the conditional probability of V given a specific U threshold is computed using:

$$P(V \leq v|U = u) = \frac{\partial C(u, v)}{\partial u} \tag{5}$$

This step quantifies the likelihood of exceeding certain rockfall volumes under given rainfall conditions, providing a probabilistic framework for hazard assessment.

3 APPLICATION

The coastal cliffs of Susan Gilmore Beach in Newcastle, NSW, Australia, were selected as the study site to assess the dependency between rockfall volume and rainfall using the copula approach. The cliffs at Susan Gilmore Beach belong to the Newcastle Coal Measures of the Sydney Basin and consist of Late Permian-aged sedimentary rocks. The lithology includes sandstone, siltstone, shale, conglomerate, and coal seams, with key stratigraphic units such as the Dudley Coal Seam, Bogey Hole Formation, Yard Coal Seam, Bar Beach Formation, and Tighes Hill Formation (Watman et al., 2023). The rock mass exhibits a blocky structure due to near-vertical joint sets and horizontal bedding planes, contributing to its instability. Weathering and erosion of weaker fine-grained layers, such as shale and siltstone, lead to the undercutting of more resistant sandstone and conglomerate, increasing the likelihood of rockfalls (see

Figure 2).

Watman et al. (2023) conducted a study on the Susan Gilmore cliff, in which the structural controls on rockfall susceptibility were characterised through geostructural mapping using Sirovision (Datamine, 2022). Structural mapping revealed a total of 1,576 discontinuities across the cliff. Three principal sets of near-vertical joints and a distinct set of nearly horizontal bedding planes were identified throughout the entire cliff (Figure 3a).

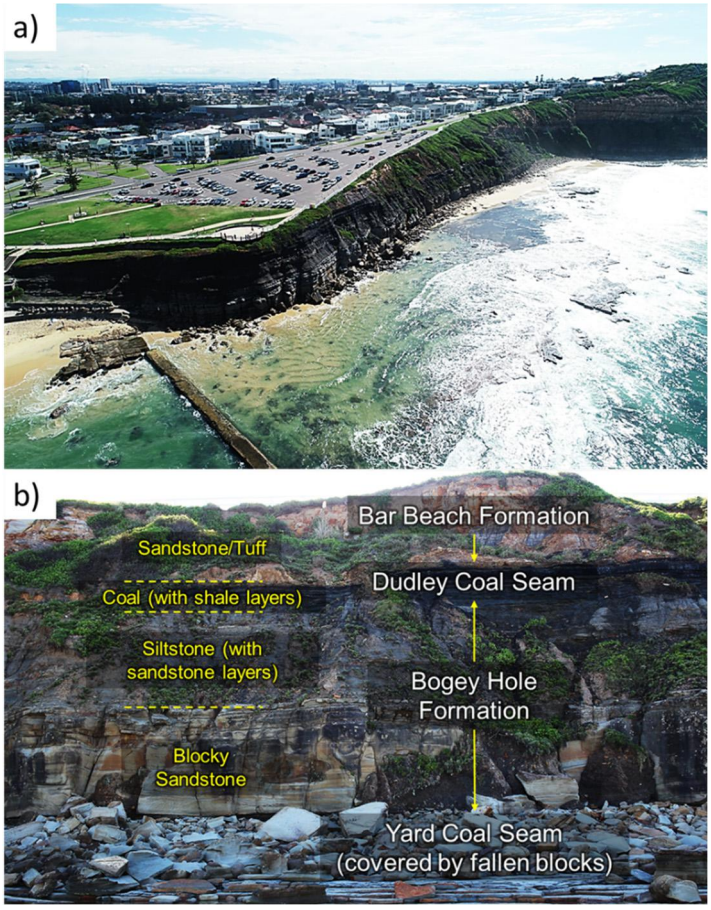

Figure 2. a) Panoramic view and b) stratigraphic units outcropping along Susan Gilmore cliff photo, modified after Watman et al. (2023).

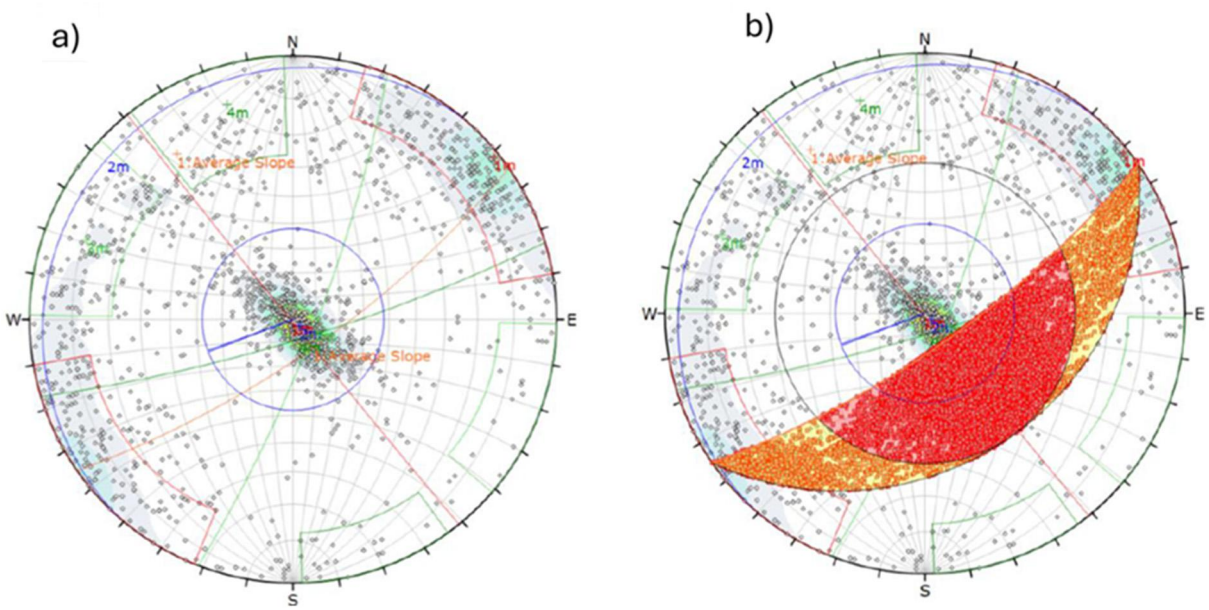

Figure 3. a) Overall stereonet and b) results from kinematic analysis for wedge sliding along the entire cliff, modified after Watman et al. (2023).

Figure 3a and Table 2 indicate three prominent near-vertical joint sets (89/231, 81/163 and 80/111), along with the set of near-horizontal bedding planes (4/311). The evaluation of the overall stereonet (Figure 3a) reveals that the possible rockfall failure mode of the cliff is direct toppling, wedge sliding and planar sliding. Kinematic analysis was performed

for the overall stereonet. The Dips output for wedge sliding is shown in Figure 3b. Besides wedge sliding, analyses were conducted for direct toppling, planar sliding, and flexural toppling. The findings from these analyses are summarised in Table 3. This table indicates that wedge sliding is the most likely failure mode for the given cliff, accounting for 13.9% of potential failures, followed by direct toppling at 6.8%, and planar sliding at 5.8%.

Table 2. Summary of orientations of structures at Susan Gilmore Beach cliff, modified after Watman et al. (2023).

set	Dip [°]	Dip Direction [°]
Red (joints)	89	231
Pale green (joints)	80	111
Dark green (joints)	81	163
Blue (bedding)	4	311
Slope	75	145

Table 3. Summary of kinematic analysis results, modified after Watman et al. (2023).

Failure Mode	Critical Intersections/ Poles	Total Intersections/ Poles	Critical Proportion [%]
Wedge Sliding	172,204	1241005	13.9
Direct Toppling	84,027	1241005	6.8
Planar Sliding	92	1576	5.8
Flexural Toppling	29	1576	1.8

3.1 DATA COLLECTION

To develop the dataset for analysis, rockfall events and rainfall measurements were recorded over a monitoring period from November 17, 2022, to November 27, 2024, during which the cliffs were surveyed 28 times at irregular intervals. Table A1 in APPENDIX A provides the monitoring intervals. Rockfall detection and volume estimation were conducted using drone-based photogrammetry. Geospatial data acquisition involved using a DJI Phantom 4 RTK drone for high-resolution aerial imaging. These datasets were processed into 3D mesh models to facilitate change detection analysis. Rockfall source areas and volumetric changes were identified using CloudCompare (Girardeau-Montaut, 2020) plug-in called "VoxFall" recently developed by the authors (Farmakis et al., 2025). Figure 4 demonstrates the cumulative frequency and magnitude (block volume) relationship of the data obtained from the 2-year observation. Note that the frequency has been normalised by the year. The figure also shows that a power-law distribution fits the observed data quite well. Furthermore, the Rainfall data was obtained from the Bureau of Meteorology (BoM), Newcastle Nobbys Signal Station AWS.

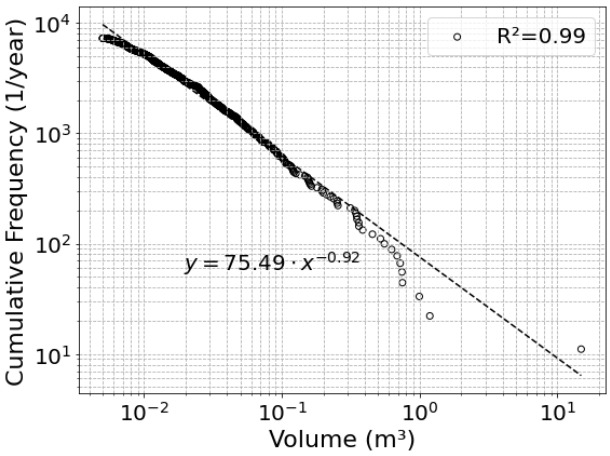

Figure 4. Relationships between the annual cumulative frequency and magnitude in a log-log plot.

3.2 DATA PREPROCESSING

As the exact timing of rockfall events was unknown within each monitoring period, a statistical approach was used to represent rockfall volume and rainfall. The 75th percentile of rockfall volume was selected to characterise the upper range

of observed events, ensuring that significant occurrences were captured. This value was then correlated with the 75th percentile of daily rainfall recorded in the same period, providing a representative dataset for analysis. The 75th percentile was selected to emphasise larger rockfall events and higher rainfall intensities, as these more hazardous occurrences are critical for risk mitigation and infrastructure planning, ensuring that preventive measures are designed for significant, rather than minor, fluctuations (Liu et al., 2022). Figure 5 and Figure 6 illustrate these distributions using box plots of rockfall volume and rainfall across all monitoring periods. Figure 7 presents the 75th percentile rockfall volume (m^3) and 75th percentile rainfall (mm) across monitoring periods, illustrating potential correlations between rainfall intensity and rockfall occurrences, with rockfall data represented as log-scaled bars and rainfall trends as dotted lines.

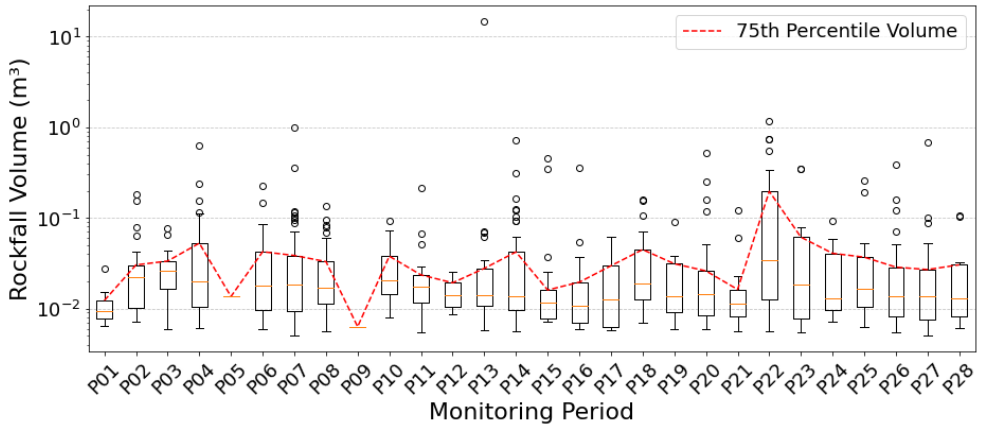

Figure 5. Boxplot of rockfall volumes across monitoring periods, with the 75th percentile volume shown as a red dashed line, highlighting variations in rockfall magnitude over time.

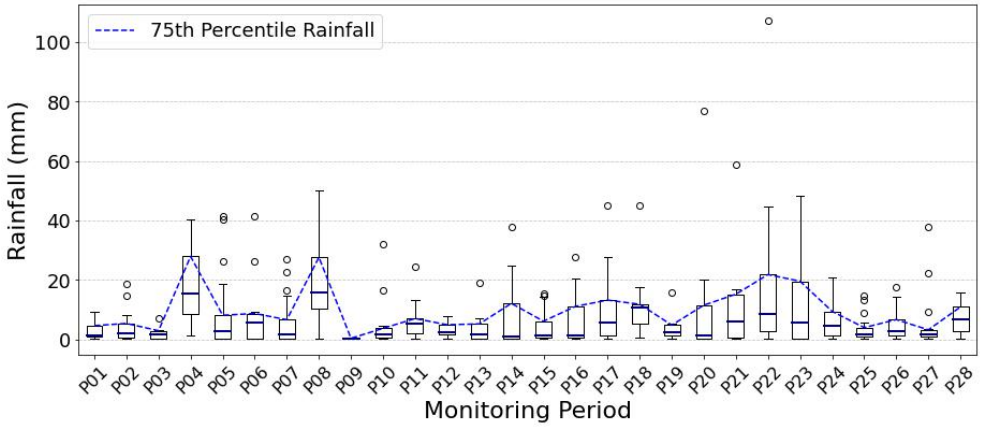

Figure 6. Boxplot of rainfall across monitoring periods, with the 75th percentile rainfall shown as a blue dashed line.

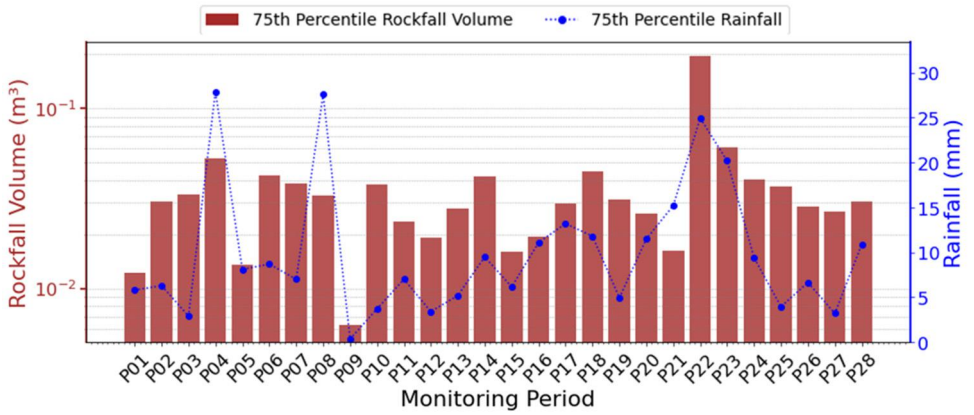

Figure 7. Comparison of 75th percentile rockfall volume and 75th percentile rainfall over monitoring periods.

After preprocessing, the dataset (28 period-wise observations of paired rockfall and rainfall values) was divided into a training subset and a testing subset in an approximately 80:20 ratio. A stratified random sampling approach (Tippett, 1931) was employed to ensure that the split was representative of the overall data distribution. In practice, this meant that

22 observations (about 80%) were randomly selected for copula model analysis, and the remaining 6 observations (about 20%) were reserved for checking the conditional probability.

4 RESULT AND DISCUSSION

4.1 EXPLORATORY DATA ANALYSIS

An exploratory data analysis was conducted to understand the underlying patterns and relationships in the training dataset, focusing on the trends, correlations and distribution between variables. The scatter plot illustrates the relationship between the rockfall volume and rainfall, with a fitted trend line indicating a positive correlation (see Figure 8). The logarithmic y-axis highlights variations in rockfall magnitude across different rainfall values. The correlation between these variables has been computed and is presented in Table 4, using Pearson's correlation and Kendall's tau. Pearson's correlation, which measures linear dependence, indicates a relatively strong relationship, while Kendall's tau, which assesses monotonic associations, suggests a moderate nonlinear trend.

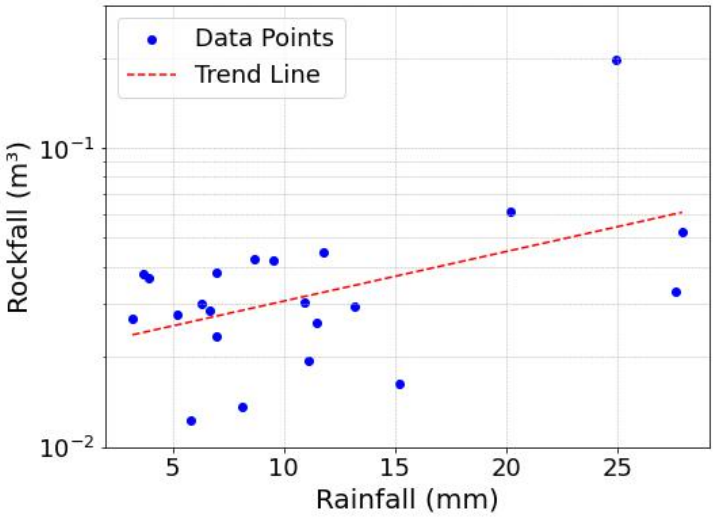

Figure 8. The scatter plot of 75th percentile rockfall volume vs. rainfall shows a moderate positive correlation with a fitted trend line.

Table 4. Pearson correlation and Kendall's tau coefficient between rockfall volume and rainfall

Pair	Pearson correlation	Kendall's tau
Rockfall-Rainfall	0.54	0.30

4.2 COPULA FITTING PROCESS

Copula fitting process starts with constructing the histograms of rockfall and rainfall to represent the frequency distribution of rockfall volume and rainfall, while ECDFs were fitted to illustrate the cumulative probability of each variable (see Figure 9). This visualisation highlights the skewness and distribution characteristics of the data, offering insights into the presence of extreme values and their potential influence on subsequent statistical modelling. Since copula modelling requires uniform marginal distributions, each variable's data was transformed using its ECDF. Figure 10 this step's result was a pseudo-observations in which rockfall and rainfall marginals were approximately uniform on the interval [0,1]. By using ECDFs, no specific parametric distribution needed to be assumed for rockfall or rainfall; the empirical distributions preserved the data characteristics and made them suitable for copula fitting.

Table 5 presents AIC and BIC Goodness-of-fit results and the copula parameter (θ) for the three Archimedean copulas (Gumbel, Clayton and Frank). The Gumbel copula exhibits the lowest AIC and BIC, indicating that it provides the best fit among the tested models. The Gumbel copula is an asymmetrical Archimedean copula known for its ability to model upper tail dependence, consistent with the expectation that extreme rainfall might strongly coincide with extreme rockfall volumes.

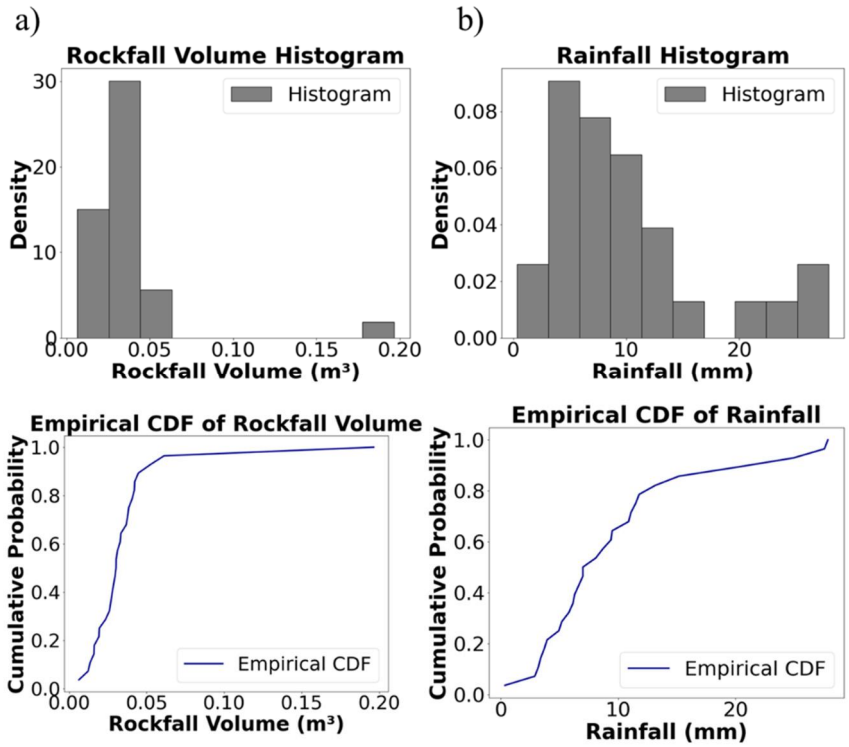

Figure 9. Histograms and ECDF of a) rockfall volume and b) rainfall, illustrating their statistical distribution and cumulative probability.

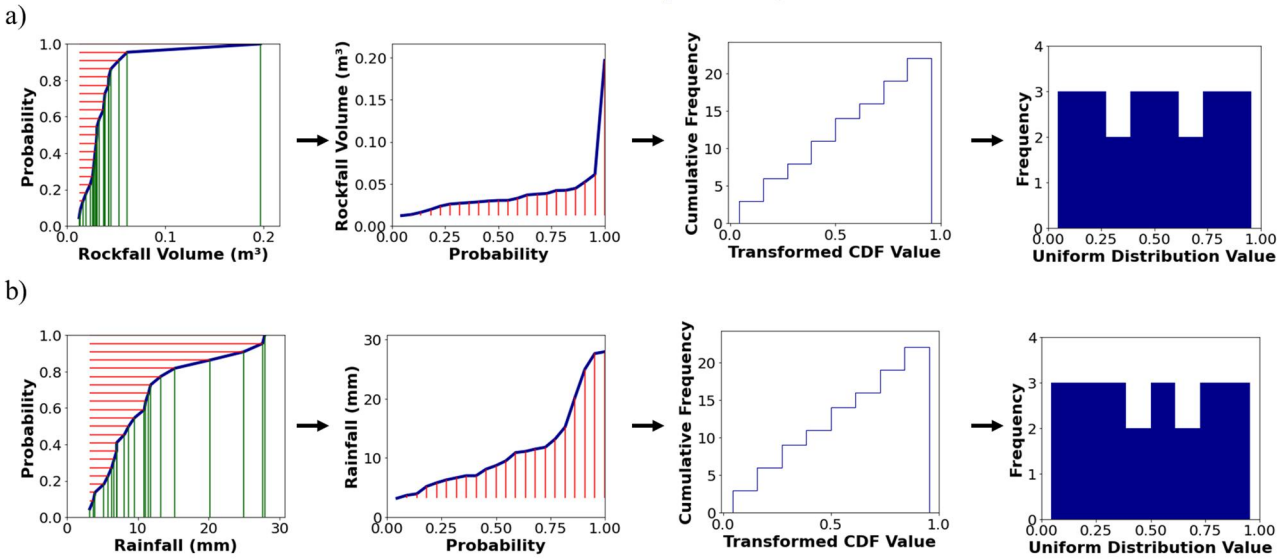

Figure 10. Transformation and uniformisation of a) rockfall volume and b) rainfall, demonstrating the mapping from the original empirical distributions to a uniform distribution through the cumulative distribution function (CDF).

Table 5. AIC and BIC values of the copula function

Copula	**AIC**	**BIC**	***θ***
Gumbel	-2.56	-4.63	1.05
Clayton	-0.88	-1.99	0.10
Frank	0.92	-1.96	50.02

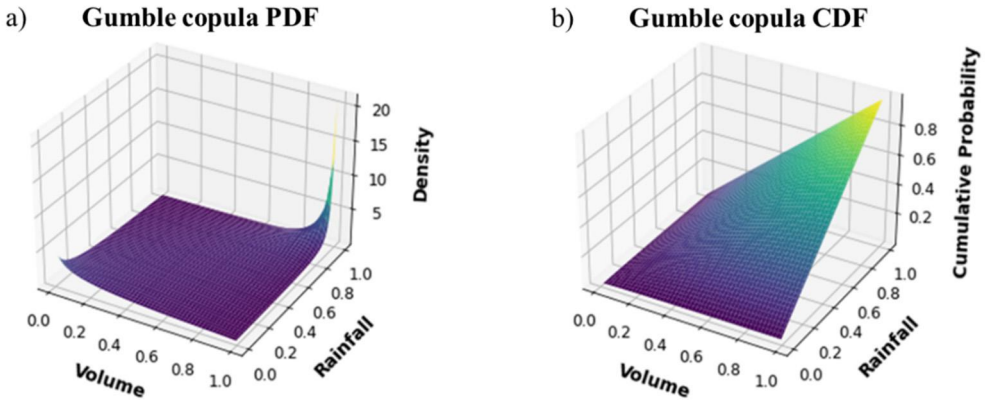

Figure 11. Gumbel copula-based Joint a) PDF and b) CDF of Rockfall Volume and Rainfall.

Following the selection of the Gumbel copula family, the process of fitting the copula to the transformed uniform data commences. Figure 11 shows the three-dimensional Gumbel copula-based joint PDF and CDF of the rockfall volume and rainfall. The concentration of density near 0 and 1 in the Gumbel copula-based joint PDF highlights a strong dependence on extreme rockfall volume and rainfall values. The high density in these regions suggests that low rainfall is typically associated with minimal rockfall activity, whereas high rainfall tends to correspond to significant rockfall events. The dependence between rockfall volume and rainfall is assessed by examining the conditional probability of volume for a given rainfall amount, as estimated from the Gumbel copula joint CDF. Figure 12 graphically demonstrates the changing conditional probability for various rockfall volumes. Each curve in the figure represents the likelihood of rockfall occurrence across various volumes corresponding to a given rainfall level. The rainfall values in Figure 12 are derived from the testing dataset and were not included in the copula-based analysis.

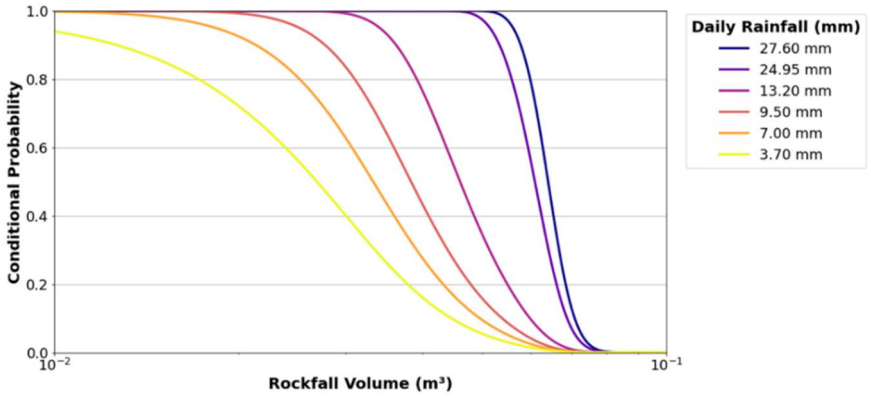

Figure 12. Conditional probabilities of the rockfall volume are given by specific amounts of rainfall.

5 CONCLUSION

This study employed a copula-based approach to investigate the relationship between rainfall and rockfall volume along the coastal cliffs of Susan Gilmore Beach, Newcastle, NSW, Australia. By utilising drone-based photogrammetry and 3D point cloud analysis, rockfall occurrences were systematically tracked over a two-year period (2022–2024), providing a detailed dataset for assessing rainfall-induced rockfall activity. Through this probabilistic modelling, the analysis captured nonlinear dependencies that traditional correlation techniques often fail to recognise, allowing for a more comprehensive understanding of how rainfall influences rockfall detachment.

The findings indicate that copula modelling is a powerful tool for estimating rockfall probability under varying rainfall conditions, as it provides greater flexibility in capturing complex relationships beyond linear assumptions. The integration of conditional probability functions enhances the ability to predict rockfall likelihood with reduced uncertainty, particularly in high-rainfall scenarios where traditional models struggle to account for variability in detachment patterns. Additionally, the conditional probability function P(V|U) derived from our copula model quantifies the likelihood of specific rockfall volumes for given rainfall amounts, enabling the definition of risk thresholds and informing targeted mitigation strategies. Furthermore, high-resolution 3D change detection methods have enabled a more accurate representation of rockfall source areas and volume changes, reinforcing the effectiveness of combining geospatial monitoring with statistical modelling in hazard assessment.

This research underscores the need for advanced analytical methods in understanding rainfall-driven rockfall processes, particularly in unstable coastal environments. The outcomes emphasise the importance of integrating meteorological data with real-time monitoring to improve hazard assessment strategies and inform risk management decisions. Expanding the

dataset with real-time monitoring systems and applying machine learning techniques could further refine predictive capabilities, contributing to more effective hazard mitigation in vulnerable coastal regions.

ACKNOWLEDGEMENTS

This work was supported by the Australian Research Council (DP210101122).

APPENDIX A

Table A1. Monitoring periods with start and end dates, and duration in days.

Monitoring Period	Start Date	End Date	Day Number	Monitoring Period	Start Date	End Date	Day Number
P01	17/11/2022	16/12/2022	29	P15	30/11/2023	9/01/2024	40
P02	16/12/2022	23/01/2023	38	P16	9/01/2024	5/02/2024	27
P03	23/01/2023	21/02/2023	29	P17	9/01/2024	22/02/2024	44
P04	21/02/2023	3/03/2023	10	P18	5/02/2024	22/02/2024	17
P05	16/12/2022	31/03/2023	105	P19	22/02/2024	28/03/2024	35
P06	3/03/2023	31/03/2023	28	P20	28/03/2024	8/04/2024	11
P07	31/03/2023	16/05/2023	46	P21	8/04/2024	24/04/2024	16
P08	16/05/2023	31/05/2023	15	P22	24/04/2024	27/05/2024	33
P09	31/05/2023	21/06/2023	21	P23	27/05/2024	26/06/2024	30
P10	21/06/2023	27/07/2023	36	P24	26/06/2024	25/07/2024	29
P11	27/07/2023	29/08/2023	33	P25	25/07/2024	29/08/2024	35
P12	29/08/2023	28/09/2023	30	P26	29/08/2024	1/10/2024	33
P13	28/09/2023	31/10/2023	33	P27	1/10/2024	31/10/2024	30
P14	31/10/2023	30/11/2023	30	P28	31/10/2024	27/11/2024	27

REFERENCES

Akaike, H. (1974). A new look at the statistical model identification. *IEEE transactions on automatic control,* 19**,** 716-723.

Ansari, M., Ahmed, M., Rajesh Singh, T. & Ghalayani, I.(2015). Rainfall, a major cause for rockfall hazard along the roadways, highways and railways on hilly terrains in India. *Engineering Geology for Society and Territory-Volume 1: Climate Change and Engineering Geology*, 2015. Springer, 457-460.

Bahootoroody, F., Giacomini, A., Guccione, D., Thoeni, K., Watman, A. & Griffiths, D. V. (2025). Predictive modelling of rainfall-induced rockfall: a copula-based approach - under review. *Georisk: Assessment and Management of Risk for Engineered Systems and Geohazards (Under Review)*.

Bajni, G., Camera, C. a. S. & Apuani, T. (2021). Deciphering meteorological influencing factors for Alpine rockfalls: a case study in Aosta Valley. *Landslides,* 18**,** 3279-3298.

Bedford, T. & Cooke, R. M. (2001). Probability density decomposition for conditionally dependent random variables modeled by vines. *Annals of Mathematics and Artificial Intelligence,* 32**,** 245-268.

Bernards, R., Van Westering, W., Morren, J. & Slootweg, H. (2020). Analysis of energy transition impact on the low-voltage network using stochastic load and generation models. *Energies,* 13**,** 6097.

Birien, T. & Gauthier, F. (2023). Assessing the relationship between weather conditions and rockfall using terrestrial laser scanning to improve risk management. *Natural Hazards and Earth System Sciences,* 23**,** 343-360.

Contino, A., Bova, P., Esposito, G., Giuffré, I. & Monteleone, S. (2017). Historical analysis of rainfall-triggered rockfalls: the case study of the disaster of the ancient hydrothermal Sclafani Spa (Madonie Mts, northern-central Sicily, Italy) in 1851. *Natural Hazards and Earth System Sciences,* 17**,** 2229-2243.

Datamine (2022). Sirovision Software 6.2.2. Australia.

Delonca, A., Gunzburger, Y. & Verdel, T. (2014). Statistical correlation between meteorological and rockfall databases. *Natural Hazards and Earth System Sciences,* 14**,** 1953-1964.

Embrechts, P., Lindskog, F. & Mcneil, A. (2001). Modelling dependence with copulas. *Rapport technique, Département de mathématiques, Institut Fédéral de Technologie de Zurich, Zurich,* 14**,** 1-50.

Farmakis, I., Guccione, D. E., Thoeni, K. & Giacomini, A. (2025). VoxFall: Non-parametric volumetric change detection for rockfalls. *Engineering Geology,* 352**,** 108045.

Genest, C. & Favre, A.-C. (2007). Everything you always wanted to know about copula modeling but were afraid to ask. *Journal of hydrologic engineering,* 12**,** 347-368.

Girardeau-Montaut, D. (2020). CloudCompare (2.11.3) . [Software].
Hashemi, S. J., Ahmed, S. & Khan, F. I. (2015). Correlation and Dependency in Multivariate Process Risk Assessment. *IFAC-PapersOnLine,* 48**,** 1339-1344.
Hazra, A. & Gogtay, N. (2016). Biostatistics series module 6: correlation and linear regression. *Indian journal of dermatology,* 61**,** 593-601.
Kendall, M. G. (1938). A new measure of rank correlation. *Biometrika,* 30**,** 81-93.
Leyva, S., Cruz-Pérez, N., Rodríguez-Martín, J., Miklin, L. & Santamarta, J. C. (2022). Rockfall and Rainfall Correlation in the Anaga Nature Reserve in Tenerife (Canary Islands, Spain). *Rock Mechanics and Rock Engineering,* 55**,** 2173-2181.
Li, H., Xu, Q., He, Y. & Deng, J. (2018). Prediction of landslide displacement with an ensemble-based extreme learning machine and copula models. *Landslides,* 15**,** 2047-2059.
Liu, T., Mcguire, L. A., Oakley, N. & Cannon, F. (2022). Temporal changes in rainfall intensity–duration thresholds for post-wildfire flash floods in southern California. *Natural Hazards and Earth System Sciences,* 22**,** 361-376.
Ma, M.-W., Ren, L.-L., Song, S.-B., Song, J.-L. & Jiang, S.-H. (2013). Goodness-of-fit tests for multi-dimensional copulas: Expanding application to historical drought data. *Water Science and Engineering,* 6**,** 18-30.
Malsam, A. & Walton, G. (2024). Seasonality of rockfall triggers and conditioning factors interpreted from a lidar-derived rockfall database. *Engineering Geology,* 333**,** 107500.
Matsuoka, N. (2019). A multi-method monitoring of timing, magnitude and origin of rockfall activity in the Japanese Alps. *Geomorphology,* 336**,** 65-76.
Melillo, M., Gariano, S. L., Peruccacci, S., Sarro, R., Mateos, R. M. & Brunetti, M. T. (2020). Rainfall and rockfalls in the Canary Islands: assessing a seasonal link. *Natural Hazards and Earth System Sciences Discussions,* 2020**,** 1-26.
Mirhadi, N. & Macciotta, R. (2023). Quantitative correlation between rock fall and weather seasonality to predict changes in rock fall hazard with climate change. *Landslides,* 20**,** 2227-2241.
Motamedi, M. & Liang, R. Y. (2014). Probabilistic landslide hazard assessment using Copula modeling technique. *Landslides,* 11**,** 565-573.
Nelsen, R. B. (2007). An introduction to copulas, *Springer science & business media*.
Ningrum, O. W., Tarno, T. & Di Asih, I. M. (2017). Perhitungan Value at Risk Pada Portofolio Saham Menggunakan Copula (Studi Kasus: Saham-Saham Perusahaan Di Indonesia Periode 13 Oktober 2011-12 Oktober 2016). *Jurnal Gaussian,* 6**,** 231-240.
Nissen, K. M., Rupp, S., Kreuzer, T., Guse, B., Damm, B. & Ulbrich, U. (2021). Quantification of Meteorological Conditions for Rockfall Triggers in Central Europe.
Papaefthymiou, G. & Kurowicka, D. (2009). Using Copulas for Modeling Stochastic Dependence in Power System Uncertainty Analysis. *IEEE Transactions on Power Systems,* 24**,** 40-49.
Parzen, E. (1962). On estimation of a probability density function and mode. *The annals of mathematical statistics,* 33**,** 1065-1076.
Schirmacher, D. & Schirmacher, E. (2008). Multivariate dependence modeling using pair-copulas. Technical report.
Schober, P., Boer, C. & Schwarte, L. A. (2018). Correlation Coefficients: Appropriate Use and Interpretation. *Anesthesia & Analgesia,* 126**,** 1763-1768.
Schoelzel, C. & Friederichs, P. (2008). Multivariate non-normally distributed random variables in climate research–introduction to the copula approach. *Nonlinear Processes in Geophysics,* 15**,** 761-772.
Schwarz, G. (1978). Estimating the dimension of a model. *The annals of statistics***,** 461-464.
Sepúlveda-García, J. J. & Alvarez, D. A. (2022). On the use of copulas in geotechnical engineering: a tutorial and state-of-the-art-review. *Archives of Computational Methods in Engineering,* 29**,** 4683-4733.
Sklar, A. (1959). Fonctions de répartition à n dimensions et leurs marges. *Publications de l'Institut de Statistique de l'Université de Paris,* 8.
Tippett, L. H. C. (1931). The Methods of Statistics*,* London, UK, *Williams & Norgate*.
Vessia, G., Di Curzio, D., Chiaudani, A. & Rusi, S. (2020). Regional rainfall threshold maps drawn through multivariate geostatistical techniques for shallow landslide hazard zonation. *Science of the Total Environment,* 705**,** 135815.
Villarini, G., Serinaldi, F. & Krajewski, W. F. (2008). Modeling radar-rainfall estimation uncertainties using parametric and non-parametric approaches. *Advances in Water Resources,* 31**,** 1674-1686.
Wang, F. & Li, H. (2018). The role of copulas in random fields: characterization and application. *Structural Safety,* 75**,** 75-88.
Wang, Y., Li, C., Liu, J., Yu, F., Qiu, Q., Tian, J. & Zhang, M. (2017). Multivariate Analysis of Joint Probability of Different Rainfall Frequencies Based on Copulas. *Water,* 9**,** 198.
Watman, A., Guccione, D. E. & Bahootoroody, F. T., K. Giacomini, A. (2023). Rockfall instability analysis of coastal cliffs: A case study along Susan Gilmore Beach (Newcastle, NSW). *14th Australia and New Zealand Conference on Geomechanics (ANZ2023).* Cairns.
Wu, X. Z. (2015). Modelling dependence structures of soil shear strength data with bivariate copulas and applications to geotechnical reliability analysis. *Soils and Foundations,* 55**,** 1243-1258.
Zhang, L. & Singh, V. P. (2019). Copulas and their applications in water resources engineering*,* Cambridge, *Cambridge University Press*.